SCIENTIFIC REPORTS

OPEN

SUBJECT AREAS:
SPINTRONICS
MAGNETIC PROPERTIES AND MATERIALS

Received
3 March 2015

Accepted
13 March 2015

Published
26 May 2015

Correspondence and requests for materials should be addressed to M.H. (michel.hehn@univ-lorraine.fr)

Indirect localization of a magnetic domain wall mediated by quasi walls

D. Lacour[1], F. Montaigne[1], N. Rougemaille[2,3], R. Belkhou[4], J. Raabe[5], M. Hehn[1]*

[1]Institut Jean Lamour, Université de Lorraine, CNRS boulevard des aiguillettes, B.P. 70239, F-54506 Vandoeuvre lès Nancy Cedex, France, [2]CNRS, Inst NEEL, F-38042 Grenoble, France, [3]Univ. Grenoble Alpes, Inst NEEL, F-38042 Grenoble, France, [4]Synchrotron SOLEIL, L'Orme des Merisiers, Saint-Aubin, B.P. 48, F-91192 Gif-sur-Yvette Cedex France, [5]Paul Scherrer Institut, Villigen PSI, Switzerland.

The manipulation of magnetic domain walls in thin films and nanostructures opens new opportunities for fundamental and applied research. But controlling reliably the position of a moving domain wall still remains challenging. So far, most of the studies aimed at understanding the physics of pinning and depinning processes in the magnetic layer in which the wall moves (active layer). In these studies, the role of other magnetic layers in the stack has been often ignored. Here, we report an indirect localization process of 180° domain walls that occurs in magnetic tunnel junctions, commonly used in spintronics. Combining Scanning Transmission X-Ray Microscopy and micromagnetic simulations, magnetic configurations in *both layers* are resolved. When nucleating a 180° domain wall in the active layer, a quasi wall is created in the reference layer, atop the wall. The wall and its quasi wall must then be moved or positioned together, as a unique object. As a mutual effect, a localized change of the magnetic properties in the reference layer induces a localized quasi wall in the active layer. The two types of quasi walls are shown to be responsible for an indirect localization process of the 180° domain wall in the active layer.

For decades, magnetic domain walls (DW) have been seen as boundaries, sometimes with complex internal structure, between uniformly magnetized domains. Nowadays, they are considered as objects in their own right. Stabilizing and manipulating DWs in nanostructures through shape[1], field[2], or more recently using spin-polarized currents[3–6] became an intense field of research in the last few years[7,8]. In particular, the control of pinning and depinning processes has raised numerous fundamental questions. While depinning mechanisms are still under debate[9–11], much effort has been devoted to the realization of well-defined pinning sites, for example using notches with controlled shape and geometries[12,13], or using crystalline defects such as micro twins[9], anti-phase boundaries, or edge roughness. Most of the time, these pinning sites are located in the magnetic layer in which the DW moves. However, many studies investigate the properties of more complex multilayer nanostructures, in which at least an active (often soft) and a reference (often hard) magnetic layer coexist. For instance, using magnetoresistive effects in bilayers and multilayers, both signal level[12,14,15] and spin torque efficiency[16] can be increased. In soft/hard bilayers, the hard ferromagnetic layer used to spin polarize the current, is often at the origin of a magnetic coupling that can influence the domain wall behavior[11,17,18]. Reports on the impact of the additional layer are sparse, especially in devices with a domain wall. The non homogeneous stray field has been shown to have a strong impact on the depinning process of a single domain wall and to be an additional source of pinning[15]. In this article, we report a new localization mechanism for magnetic domain walls in layered structures.

In this work, we investigate the magnetic switching of the soft layer of a magnetic tunnel junction (MTJ) using Scanning Transmission X-ray Microscopy (STXM). An *in-situ* magnetic field has been applied on 1×3 μm^2 elliptical shaped MTJ with the following stacking: Ta(5)/Al_2O_3(2)/Co(4)/Al_2O_3(2)/$Fe_{20}Ni_{80}$(4)/Ru(2) (layer thicknesses in nanometers). To enable transmission measurements, the MTJs are fabricated by sputtering deposition and patterned on 200-nm thick Si_3N_4 membranes, the membranes being almost transparent to the soft X-rays. The micromagnetic configurations of soft layer (NiFe) and the hard layer (Co) have been imaged taking advantage of chemical selectivity of the technique and the large XMCD effect associated with respectively the Ni and the Co L_3 edges[19]. A set of XMCD-STXM images have been taken for different values of applied magnetic field, along the magnetic hysteresis curve of the soft layer (NiFe). The STXM set-up geometry has been chosen in order to probe predominantly the in-plane component of the magnetization, along the ellipses axis (easy magnetic direction). XMCD-STXM images obtained for different magnetic fields recorded at the Ni edge are shown in Fig. 1. Two typical cases are represented in Fig. 1a and Fig. 1b. They correspond to two different ellipses and are characterized by the micromagnetic configuration of the soft layer at remanence. In the first configuration, as it

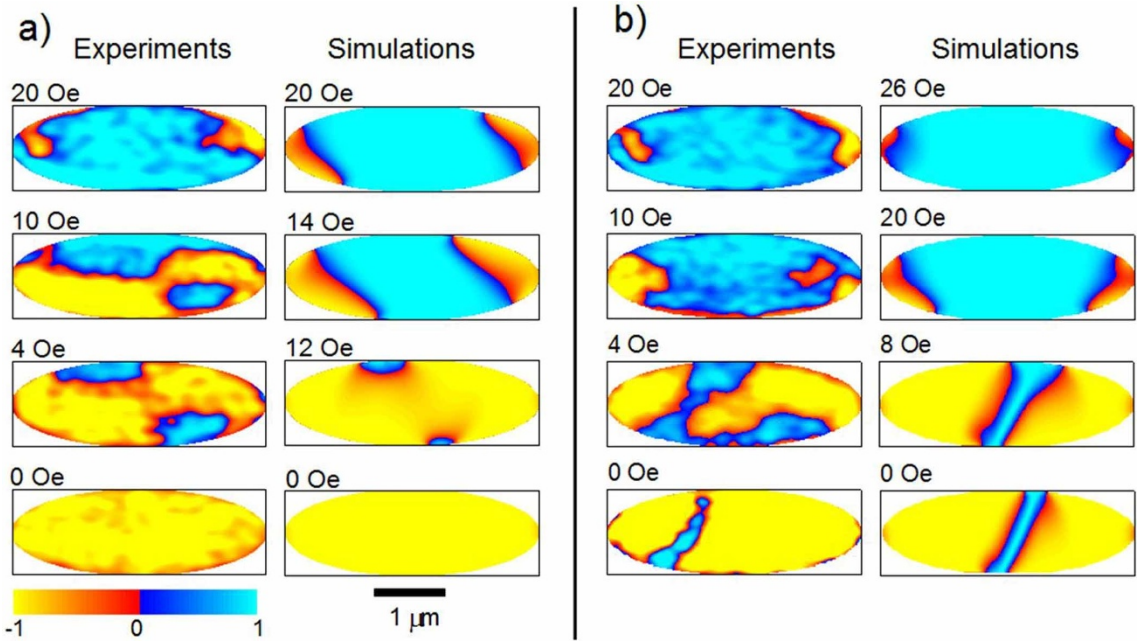

Figure 1 | XMCD-STXM images and simulations of the soft layer magnetic configuration. Experimental images and simulations are recorded for different value of magnetic applied field after saturation in a positive field. In each case the reversal process is initiated by domain nucleations at the ellipses extremities**.** While the magnetic states of the soft layer is mostly uniform at 0 Oe in the case (a) a 360° DW is present in the case presented in (b). The color level corresponds to the in-plane projection of the magnetization along the long ellipse axis. The magnetization is normalized w.r.t. saturation magnetization.

can be seen on Fig. 1a (0 Oe), the magnetic state is mostly uniform. This contrasts with the second case reported in Fig. 1b (0 Oe) where the soft layer hosts a 360° DW. The observed drastic difference has been ascribed to a reversal process taking place at the ellipses extremities[18] induced by the dipolar stray field originating from the Co hard layer. To unveil the magnetic switching process of the NiFe soft layer, the STXM setup was used with an *in-situ* applied field. First, the sample is saturated with a 1 kOe field applied along the ellipses' long axis: both the NiFe soft layer and the Co hard layer align their magnetization along the field direction and exhibit a single domain state. The soft layer magnetic state is then imaged decreasing the applied field (20, 10, 4 and 0 Oe). In both cases (Fig. 1a and 1b) domain nucleations occur at the extremities of the ellipses for positive field values (Fig. 1: 20 Oe). The anticipated reversal (*i.e.* for positive field values) of the soft layer magnetization is an effect of the stray field originating from the Co layer at the ellipses' edges. A further reduction of the field leads to the propagation of the previously nucleated domains towards the ellipses core (Fig. 1: 10 and 4 Oe). These observations reveal unambiguously the reversal process originating from the ellipses extremities.

To gain more insight into the reversal mechanism that leads to the formation or non-formation of a 360° DW, micromagnetic calculations were conducted[20]. In the initial state, both layers are saturated by applying a magnetic field along to the long axis of the ellipse. Then, the field is progressively reduced to zero. As the applied field is lowered, the torque exerted by the stray field originating from the hard layer leads to the nucleation of reversed domains in the soft layer, at the ellipse extremities (Fig. 1b 26 and 20 Oe).

The two resulting 180° DWs further propagate towards the center of the ellipse where they meet. If the two DWs have the same chirality, a 360° DW forms, while these two walls annihilate each other if they have opposite chirality. The case where the 360° DW collapses is well reproduced by introducing in the simulation a local tilt of the anisotropy direction at one of the ellipse extremities (10° w.r.t the long axis) to select the desired chirality of the nucleated 180° DW. Thus, the formation or collapsing of a 360° DW is triggered by the relative chirality of the two 180° DW, nucleated at the ellipse extremities.

However, numerical simulations always predict a localization of the 360° DW at the ellipse' center, while this is only rarely observed in our measurements. The capability of the XMCD-STXM technique to probe the two ferromagnetic layers independently, provides valuable information to unveil the driving mechanism leading to the localization of the 360° DW. The micromagnetic configuration of both layers could be imaged on the same ellipses, during the magnetic field sequence, as shown in Fig. 2. To do so, images are recorded at the Ni and Co edges after saturation with a 1 kOe field applied along the long axis of the ellipses. Then, the applied field is reduced down to zero. Here again the magnetic contrast corresponds to the magnetization component parallel to the long axis of the ellipses. It is worth noticing that the magnetization in the hard layer is not uniform. In particular, for a 20 Oe applied field, a localized magnetization inhomogeneity is observed in the hard layer, while no DW is present on top of it in the soft layer (Fig. 2a). This inhomogeneity corresponds to a reduction of about 20% of the in-plane magnetization component along the long axis of the ellipse. A further decrease of the field to 10 Oe leads to the localization of a 180° DW at a position slightly shifted to the right from the top of this inhomogeneity (Fig. 2a, 10 Oe). Then at zero applied field, both 180° DWs have met, forming the 360° DW localized atop the magnetic inhomogeneity in the hard layer (Fig. 2a, 0 Oe). The magnetization profiles extracted from the zero field images in both layers confirm that the 360° DW position is aligned but slightly shifted to the right from the magnetization inhomogeneity observed in the hard layer (see Fig. 2c). This phenomenon has been observed on 3 different ellipses and appears to be systematic.

Micromagnetic calculations taking into account a local tilt of anisotropy (or fluctuation of anisotropy) with a higher anisotropy value in the hard layer present a very good agreement with the experimental observations (Fig. 2c and supplemental material). The spatially localized change of the magnetic property of the hard layer creates a pinning site position for a 180° DW and imposes the location of the 360° DW (Fig. 2b and 2c). At this point the physical nature of the interaction between the hard layer fluctuation and the 180° DWs in the soft layer remains to be unveiled.

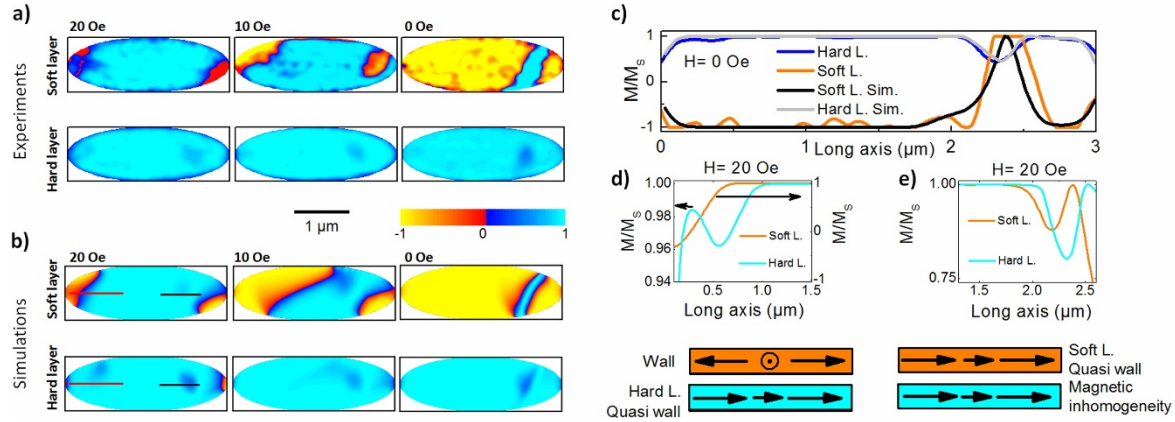

Figure 2 | (a) XMCD-STXM images. The magnetic configurations of the soft and hard layers have been recorded on one typical ellipse as a function of the applied field after saturation at high positive field. When the field is reduced to zero a 360° DW is formed in the soft layer on top of a localized inhomogeneity of magnetization present in the hard layer; (b) Computed micromagnetic configurations of the soft and hard layers as a function of applied field. The simulation takes into account a local tilt of anisotropy with higher anisotropy value in the hard layer at the position corresponding to the spatial inhomogeneity of magnetization observed experimentally; (c) Magnetization profiles in the soft and hard layers extracted from both the experimental images and simulations; (d) Profiles of a 180° wall (orange line) in the soft layer associated with its quasi wall (cyan line) in the hard layer. Both profiles are extracted from the simulated micromagnetic configuration corresponding to a 20 Oe field (see red line on fig b 20 Oe); Schematic representation of the wall / quasi wall couple; e) Profiles of the Co inhomogeneity in the hard layer (cyan line) with its associated quasi wall (orange line) in the NiFe soft layer. Both profiles are extracted from the simulated micromagnetic configuration corresponding to a 20 Oe field (see black line in fig b 20 Oe); Schematic representation of the fluctuation / quasi wall couple.

When two magnetic layers are separated by a thin non magnetic layer, and when one of the layers hosts a 180° DW, the magnetostatic energy of the system is reduced by the formation of a magnetic quasi-wall, QDW, in the other layer[21–23]. In other words, the quasi-wall partly screens the magnetic charges of the domain walls. In our micromagnetic simulations, a quasi-wall is indeed observed in the hard layer, corresponding to a local rotation of the hard layer magnetization by few degrees, following the motion of the 180° DW in the soft layer (see Fig. 2d). Similarly, the local fluctuation of the anisotropy in the hard layer leads to the formation of another quasi-wall in the soft layer. In the following, we will call this quasi-wall a 'quasi-fluctuation', since created through dipolar coupling by the fluctuation of magnetization in the hard layer. Considering only one of the two nucleated 180° DWs, our system is then described by one 180° DW in the soft layer, one region of tilted magnetization in the hard layer created by a local tilt of the magnetic anisotropy, one quasi-wall and one quasi-fluctuation (Fig. 3a). This situation is more complex than the one observed when the 180° DW and the fluctuation are only coupled by dipolar coupling, direct coupling that is here reduced by the flux closure in the DW / QDW and the fluctuation / quasi-fluctuation subsystems.

To highlight the role of the quasi-wall and the quasi-fluctuation in the pinning process of 180° domain walls in magnetic multilayers, we have conducted dedicated micromagnetic calculations. In a first set of simulations, we artificially stopped the quasi-wall motion by freezing the magnetic configuration in the Co hard layer, leaving only the soft layer free to evolve. We observe that the 180° DW stays on top of its frozen quasi-wall: any object that pins, without deformation, the quasi-wall in the Co layer thus also pins the 180° DW in the soft layer. In a second set of micromagnetic calculation, we have artificially

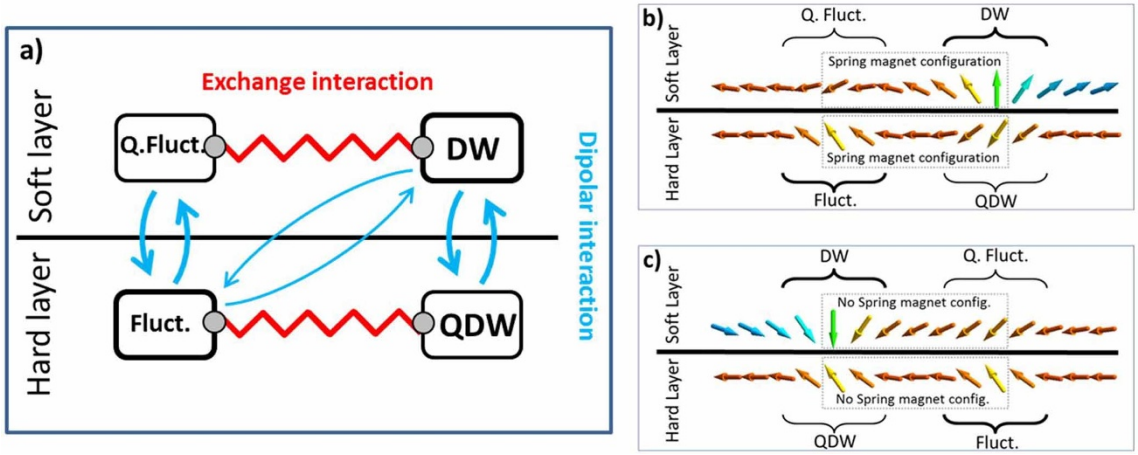

Figure 3 | (a) Interactions diagram between one 180° DW in the soft layer (DW), a fluctuation in the hard layer (Fluct), their associated quasi domain wall (QDW) and quasi fluctuation (Q. Fluct) respectively; (b) One dimensional sketch of the magnetizations in the soft (top) and hard (bottom) magnetic layers when a domain wall is nucleated at the right of the ellipse as in the STXM images. The magnetization in the hard layer inhomogeneity induces in both magnetic layers a spring magnet type configuration that stops the propagation of the 180° domain wall in the soft layer; (c) One dimensional sketch of the magnetizations in the soft (top) and hard (bottom) magnetic layers when a domain wall is nucleated at the left of the ellipse as in the STXM images. The magnetization in the hard layer inhomogeneity does not induce a spring magnet type configuration in the layers and the 180° domain wall in the soft layer propagates through the magnetic inhomogeneity.

frozen the quasi-fluctuation in the soft layer and removed the inhomogeneity region in the Co hard layer and so its stray field. This also leads to the localization of the 180° DW in the soft layer and of its associated quasi-wall in the hard layer. The existence of the quasi-wall and the quasi-fluctuation are the key to explain the pinning process. However, why does the second 180° DW nucleated at the other ellipse extremity propagates though the hard layer magnetization fluctuation region?

Lets first consider the 180° DW nucleated at the right end of the ellipse. As shown in Fig. 3b, in the soft layer, the 180° DW meets the quasi-fluctuation induced by the localized fluctuation in the hard layer: their magnetization are antiparallel; This configuration, we call 'lateral spring magnet configuration', prevents the propagation of the 180° DW since the compression of this spring will lead to an increase of the exchange energy like it is in a conventional domain wall under applied field. In the hard layer, the quasi-wall induced by the 180° DW meets the localized magnetization fluctuation; their magnetization are also antiparallel and a lateral spring magnet configuration is also developed. In order to propagate the 180° DW, both spring magnet configurations have to unwind. This happens when the anisotropy of the magnetic inhomogeneity is small or when the magnetization in the hard layer fluctuation is oriented close to the long ellipse axis (see sup. Material). On the other hand, as shown in Fig. 3c, the 180° DW nucleated at the other extremity in the soft layer has its magnetization parallel to the quasi-fluctuation and the magnetizations, in the hard layer, of the quasi-wall induced by the 180° DW and of the localized fluctuation are also parallel. As a result, the 180° DW propagates and the two DWs then meet at the vicinity of the magnetic inhomogeneity in the hard layer where they localize, slightly shifter towards the right of the defect where the other DW has stopped.

In summary, we showed in this study that quasi walls can play a key role in the pinning processes of DWs in magnetic multilayers. This new mechanism is of primary importance in the context of intense research on domain walls manipulation, and should be at work in most of the systems where quasi walls are present and where quasi walls could be blocked or could act as blocking sites.

METHODS

Sample fabrication. The MTJ multilayer stack was grown in a UHV Alliance Concept sputtering system on a 200 nm thick Si_3N_4 (NTT, Japan) membrane in order to allow STXM experiments. The sample is composed of membrane//Ta(5)/AlO3(2)/Co(4)/Al2O3(2)/Fe20Ni80(4)/Ru(2) (layer thicknesses in nanometers). The coercive fields of the continuous Co and NiFe are, respectively, 50 and 20 Oe. The ferromagnetic coupling field between the two layers is less than 5 Oe. 1 × 3 μm2 ellipses have been patterned by electron beam lithography using a JEOL 6500F scanning electron microscope. These structures are defined using an Al mask and a subsequent Ar ion beam etching down to the Si_3N_4 substrate.

STXM measurements. The measurements have been performed at the POLLUX beamline[24] on the Swiss Light Source synchrotron (SLS-Villigen, Switzerland). The magnetic domain images have been recorded using a soft X-ray transmission STXM microscope (Scanning Transmission X-ray Microscope). In the microscope setup, the X-ray beam can be focused down to 14 nm[25] spot size using diffractive zone plate lenses. For these experiments, a typical 40 nm beam spot has been used in order to optimise the signal to background level and the efficiency of the zone plate. The images were recorded scanning the beam through the sample and collecting the X-ray absorption signal using a photomultiplier tube with a phosphor scintillator. We took benefit from the chemical sensitivity of the X-ray Absorption Spectroscopy (XAS) to selectively image both electrodes of the MTJ. The Co hard layer was imaged using the Co L_3 (777 eV) absorption edges, while the soft NiFe was investigated using the Ni L_3 (852 eV) edge. The magnetic domain configuration of each layer has been investigated taking advantage of the large circular dichroism signal associated with the Co and Ni L edge at circular left/right X-ray polarization. The beam incidence was set at 30° of sample normal to image predominantly the in-plane magnetic domain. For each absorption edge, a set of two images has been recorded with respectively right and left circular polarisation. The difference image gives access directly to the onset of the magnetic domain as shown in the figures. The yellow areas correspond to domain with magnetization antiparallel to the light direction, meanwhile the blue onbes correspond to the opposite magnetization. Finally the measurements have been done under an applied magnetic field following the magnetization curve of both hard and soft layer.

Micromagnetic calculations. STXM images are compared with micromagnetic calculations done using the LLG Micromagnetics SimulatorTM[20] and the OOMMF code[26] (especially for the additional materials). The uniaxial anisotropy (NiFe : 4.10^3 erg/cm^3, Co : 3.10^4 erg/cm^3) and magnetization material (NiFe : 800 emu/cm^3, Co : 1420 emu/cm^3) parameters have been extracted from magnetic measurements on full films. The cell size has been optimized to 5 nm, about 50 times lower than the extension of the observed 360° domain wall. The shape and position of the localized inhomogeneity of the reference Co layer has been extracted from the STXM. It has been modeled by a fluctuation of anisotropy with a different value of the anisotropy constant. The angle of 50° and the anisotropy value of 8.10^4 erg/cm^3 have been chosen because they reproduce the experimental magnetization variation with applied field of the Co inhomogeneity region (see additional material).

1. Hehn, M. *et al.* Nanoscale Magnetic Domains in Mesoscopic Magnets. *Science* **272**, 1782–1785 (1996).
2. Allwood, D. A. *et al.* Submicrometer Ferromagnetic NOT Gate and Shift Register. *Science* **296**, 2003–2006 (2002).
3. Grollier, J. *et al.* Switching the magnetic configuration of a spin valve by current-induced domain wall motion. *J. Appl. Phys.* **92**, 4825–4827 (2002).
4. Ravelosona, D., Lacour, D., Katine, J. A., Terris, B. D. & Chappert, C. Nanometer Scale Observation of High Efficiency Thermally Assisted Current-Driven Domain Wall Depinning. *Phys. Rev. Lett.* **95**, 117203 (2005).
5. Kläui, M. *et al.* Direct Observation of Domain-Wall Configurations Transformed by Spin Currents. *Phys. Rev. Lett.* **95**, 026601 (2005).
6. Hayashi, M. et al. Influence of Current on Field-Driven Domain Wall Motion in Permalloy Nanowires from Time Resolved Measurements of Anisotropic Magnetoresistance. *Phys. Rev. Lett.* 96, 197207 (2006).
7. Parkin, S. S. P., Hayashi, M. & Thomas, L. Magnetic Domain-Wall Racetrack Memory. *Science* **320**, 190–194 (2008).
8. Allwood, D. *et al.* Magnetic Domain-Wall Logic. *Science* **309**, 1688–1692 (2005).
9. Attané, J. P., Ravelosona, D., Marty, A., Samson, Y. & Chappert, C. Thermally Activated Depinning of a Narrow Domain Wall from a Single Defect. *Phys. Rev. Lett.* **96**, 147204 (2006).
10. Im, M.-Y., Bocklage, L., Fischer, P. & Meier, G. Direct Observation of Stochastic Domain-Wall Depinning in Magnetic Nanowires. *Phys. Rev. Lett.* **102**, 147204 (2009).
11. Hauet, T. *et al.* Direct observation of field and temperature induced domain replication in dipolar coupled perpendicular anisotropy films. *Phys. Rev. B* **77**, 184421 (2008).
12. Ono, T., Miyajima, H., Shigeto, K., Shigeto, T. & Shinjo, T. Magnetization reversal in submicron magnetic wire studied by using giant magnetoresistance effect. *Appl. Phys. Lett.* **72**, 1116–1117 (1998).
13. Kläui, M. et al. Domain Wall Pinning in Narrow Ferromagnetic Ring Structures Probed by Magnetoresistance Measurements. *Phys. Rev. Lett.* **90**, 097202 (2003).
14. Jiang, X. *et al.* Enhanced stochasticity of domain wall motion in magnetic racetracks due to dynamic pinning. *Nat. Comm.* **1**:25, DOI: 10.1038/ncomms1024 (2010).
15. Briones, J. *et al.* Magnetic domain wall propagation in a submicron spin-valve stripe: Influence of the pinned layer. *Appl. Phys. Lett.* **92**, 032508 (2008).
16. Khvalkovskiy, A. V. *et al.* High Domain Wall Velocities due to Spin Currents Perpendicular to the Plane. *Phys. Rev. Lett.* **102**, 067206 (2009).
17. Uhlíř, V. *et al.* Current-induced motion and pinning of domain walls in spin-valve nanowires studied by XMCD-PEEM. *Phys. Rev. B* **81**, 224418 (2010).
18. Hehn, M. *et al.* 360° domain wall generation in the soft layer of magnetic tunnel junctions. *Appl. Phys. Lett.* **92**, 072501 (2008).
19. Stöhr, J., Padmore, H. A., Anders, S., Stammler, T. & Scheinfein, M. R. Principles of X-Ray Magnetic Dichroism Spectromicroscopy. *Surface Review and Letters* **5**, 1297 (1998).
20. Scheinfein, M. R. *LLG Micromagnetics Simulator* (1997).
21. Middelhoek, S. Perturbation walls in thin magnetic double permalloy (Ni-Fe) films. *Appl. Phys. Lett.* **5**, 70–72 (1964).
22. Slonczewski, J. C. & Middelhoek, S. Energy of walls in thin magnetic double permally (Ni-Fe) films. *Appl. Phys. Lett.* **6**, 139–140 (1965).
23. Néel, L. Parois dans les films minces. *Journal de Physique* **29**, C2-87-C2-94 (1968).
24. Raabe, J. *et al.* PolLux: A new facility for soft x-ray spectromicroscopy at the Swiss Light Source. *Rev. of Scientific Inst.* **79**, 113704 (2008).
25. Jefimovs, K. *et al.* Zone-Doubling Technique to Produce Ultrahigh-Resolution X-Ray Optics. *Phys. Rev. Lett.* **99**, 264801 (2007).
26. Donahue, M. J. & Porter, D. G. *OOMMF user's guide version 1.0 NISTIR 6376* (Gaithersburg, MD: National Institute of Standards and Technology) (1999).

Acknowledgments

We would like to thank T. Hauet and J. Vogel for fruitful discussion and N. Foxell for technical corrections of the manuscript. This work was financially supported by La Région Lorraine. Correspondence and requests for materials should be addressed to M. H.

Author contributions

D.L., F.M., N.R., R.B., D.L., and M.H. conceived the project. M.H. was in charge of the thin films growth. F.M. structured the samples. R. B., J. R. and M.H. participate to the STXM experiments. The STXM data acquisition was performed by R. B. and J. R. M.H. and N.R. made the micromagnetic calculations. D.L. made the data treatment. F.M., D.L., N.R. and

M.H. have analyzed the results. D.L., N.R. and M.H. have written the manuscript. All the authors have discussed the results as well as this report.

Additional information

Supplementary Information accompanies this paper at http://www.nature.com/scientificreports

Competing financial interests: The authors declare that they have no competing financial interests.

How to cite this article: Lacour, D. *et al.* Indirect localization of a magnetic domain wall mediated by quasi walls. *Sci. Rep.* **5**, 9815; DOI:10.1038/srep09815 (2015).